Technical Paper

Transactions of the Society of Naval Architects of Korea
Vol. 29, No.3, August 1992
大韓造船學會論文集
第 29 卷 第 3 號 1992 年 8 月

A Finite Volume Method for Computations of Two-Dimensional Laminar Flows

by

Ki-Sup Kim* and Myung-Kyoon Chung**

이차원 층류유동 해석을 위한 유한체적법

김기섭*, 정명균**

Abstract

A Finite volume method for the computation of the two-dimensional, incompressible, steady, laminar Navier-Stokes equation is developed using a non-staggered grid system in a general curvilinear coordinate. The numerical pressure fluctuations, usually encountered when the non-staggered grid system is used, is suppressed by the momentum interpolation method. Flows around a NACA0012 foil section have been computed by the present method and the results show good agreements with other experimental and numerical ones.

요 약

2차원 비압축성, 정상, 층류 Navier-Stokes 방정식을 일반 곡선 좌표계에서 계산하기 위한 유한체적법을 개발하였다. 수치해석은 정규 격자구조를 채택하였으며, 이때 압력의 불안정한 거동은 모멘텀 보간법에 의하여 제거하였다. NACA0012 날개 단면 주위의 유동을 개발된 컴퓨터 프로그램으로 계산한 결과들은 실험 및 다른 계산결과와 잘 일치하였다.

1. Introduction

With rapid decrease in computing costs, numerical simulations of three dimensional turbulent flows around complicated geometries become popular in these days. However the basic numerical methods for those simulations are quite different for various applications. New numerical methods

발표 : 1991년도 대한조선학회 춘계연구발표회('91. 4. 13.)
Manuscript received : May 15, 1991, revised manuscript received : May 24, 1992.
* Member, Korea Research Institute of Ships & Ocean Engineering
** Dept. of Mechanical Eng., Korea Advanced Institute of Science & Technology

and solution procedures are still developing and should be verified for their reliability and efficiency for each particular application in hand. For the verification of the numerical method, a two dimensional calculation of laminar flow is still essential.

In this paper a finite volume method for the computation of the two-dimensional, incompressible, steady, laminar Navier-Stokes equation is developed using a non-staggered grid system in a general curvillinear coordinate. The flow around a NACA 0012 foil section is computed using a body-fitted grid of C-type. The numerical pressure fluctuations, usually encounted when the non-staggered grid system is used, is suppressed by the momentum interpolation method.

In the formulation for incompressible fluid flow using primitive variables, one of the most important problems is how the velocity-pressure coupling is treated. The velocity-pressure coupling should be specially considered in both the solution algorithm and the grid system used. In order to avoid the checkerboard instability in the pressure field, Hirt et al.[1] used an alternative method in which the location of pressure calculation is the center of the control volume and velocity components(u, v) are defined at the corners. Maliska and Raithby[2] stored the cartesian velocity comonents at the center of cell-face, and scalar quantities at the center of the control volumn. Both methods require a complex programming, extensive computer storage and computing time.

Gosman and Ideriah[3], and Shyy et al.[4] employed the staggered grid usually adopted in a cartesian coordinate system. Karaki and Patankar [5] used covariant velocity components as dependent variables in the momentum equations. Covariant velocity components are stored at the cell-face in staggered grid sense. The method, then, gives a diagonally dominant pressure correction equation even in a strongly non-orthogonal grid system. The success of this method largely depends on the accuracy of the adapted grid system and the manipulation of the source terms in the momentum equations. Demirdzic et al.[6] developed a calculation method in which contravariant velocity components are used as dependent variables for the momentum equations. The governing equations become extremely complicated and results of the method is quite grid dependent. However, this approach usually gives smaller numerical diffusion compared to other methods.

In non-staggered grid system, all the dependent variables are computed and stored at the center of a control volume. Cartesian velocity components are used as dependent variables in the momentum equations. This method was firstly proposed by Rhie and Chow[7] and used by Majumder[8, Miller and Schmidt[9], Peric[10] and Hsu[11]. The present study adopts this non-staggered grid system because evaluation of the curvature terms, which are extremely grid dependent, can be avoided and because a strong conservation from can be obtained. In order to avoide checkerboard pressure field, momentum interpolation method was adoped. [8], [9]. The non-staggered grid method used by Rhie and Chow[7] and Peric[10] gives a solution which depends on the under-relaxation factors[9]. Such dependence on the under-relaxation factor would certainly be undesirable feature of their method. In the present study, momentum interpolation method was used to achieve an unique solution in an iterative algorithm[8]. Computation results are compard with other numerical and experimental ones.

2. Governing Equations and Transformation

Governing Equations

A general form of the continuity equation and the transport equations for the steady, laminar flow of incompressible fluid is written as, in a cartesian tensor form,

$$\frac{\partial}{\partial xi}(\rho u_i)=0 \tag{1}$$

$$\frac{\partial}{\partial xi}(\rho u_i u_j)=-\frac{\partial p}{\partial xi}+\frac{\partial}{\partial xi}(\mu\frac{\partial u_j}{\partial xi}) \tag{2}$$

where ρ is the mean density, u the mean velocity and p the mean pressure.

Transformation of the Governing Equations

The general differential equation to obey a generalized conservation principle can be written in a two-dimensional cartesian coordinate system as follows:

$$\frac{\partial}{\partial x}(\rho u \phi)+\frac{\partial}{\partial y}(\rho v \phi)=\frac{\partial}{\partial x}(\mu\frac{\partial \phi}{\partial x})+\frac{\partial}{\partial y}+(\mu\frac{\partial \phi}{\partial y})+S_\phi \tag{3}$$

where μ is molecular viscosity, ϕ denotes arbitrary scalar dependent variables and S_ϕ denotes source terms containing the pressure term. In order to map the physical domain to the computational domain, a general transformation using new independent variables, such as $\xi(x, y)$, $\eta(x, y)$, must be adopted. Partial derivatives of any function f are transformed according to

$$f_x=(y_\eta f_\xi-y_\xi f_\eta)/J \tag{4}$$

$$f_y=(-x_\eta f_\xi+x_\xi f_\eta)/J \tag{5}$$

where the subscripts(ξ, η) on $f(=u, v)$ denote differentiation with respective to (ξ, η). J is the Jacobian of the transformation given by

$$J=x_\xi y_\eta-x_\eta y_\xi \tag{6}$$

For integrating the transformed governing differential equations over finite control volumes, the Gauss theorem is used. Upon introducing

$$\begin{aligned} U&=y_\eta u-x_\eta v \\ V&=x_\xi v-y_\xi u \\ B_1^1&=x_\eta^2+y_\eta^2 \\ B_1^2&=-(x_\xi x_\eta+y_\xi y_\eta) \\ B_2^2&=x_\xi^2+y_\xi^2, \end{aligned} \tag{7}$$

the integral from of the transformed governing equations can be written as follows.

$$\begin{aligned} &\int_{\triangle V}\frac{\partial}{\partial \xi}(\rho U \phi)d\xi d\eta+\int_{\triangle V}\frac{\partial}{\partial \eta}(\rho V \phi)d\xi d\eta \\ &=\int_{\triangle V}\frac{\partial}{\partial \xi}[\frac{\mu}{J}(B_1^1\frac{\partial \phi}{\partial \xi}+B_2^1\frac{\partial \phi}{\partial \xi})]d\xi d\eta \\ &+\int_{\triangle V}\frac{\partial}{\partial \eta}[\frac{\mu}{J}(B_1^2\frac{\partial \phi}{\partial \xi}+B_2^2\frac{\partial \phi}{\partial \eta})]d\xi d\eta \\ &+\int_{\triangle V}J\cdot S_\phi d\xi d\eta \end{aligned} \tag{8}$$

where U, V represent the convection flux in the ξ- and the η-direction, respectively.

3. Method of Numerical Computation

Discretization of the Transport Equations

In the finite volumn method[12], the governing differential equations are integrated over the control volumes with size, $\Delta\xi=\Delta\eta=1$, as shown in Fig.1.

Using the Gauss theorem, the volume integral can be converted into surface integrals along the faces of the control volume. The transport equation integrated over the control volume ΔV, enclosing node P can be expressed as:

$$I_e-I_w+I_n-I_s=\int_{\triangle V}S_\phi dV \tag{9}$$

where

$$I_e=(\rho U \phi)_e-[\frac{\mu}{J}(B_1^1\phi_\xi+B_2^1\phi_\eta)]_e$$

$$I_n=(\rho V \phi)_n-[\frac{\mu}{J}(B_1^2\phi_\xi+B_2^2\phi_\eta)]_n$$

The volumen integrals of the source terms are linearized and may therefore be evaluated as following :

$$\int_{\triangle V}S_\phi dV=S_\phi^C+\phi_p S_\phi^P\triangle V \tag{10}$$

By putting the non-orthogonal terms into source terms, Eq.(9) can be written,

$$\begin{aligned} &[\rho U\phi-\frac{\mu}{\triangle V}B_1^1\phi_\xi]_e-[\rho U\phi-\frac{\mu}{\triangle V}B_1^1\phi_\xi]_w \\ &+[\rho V\phi-\frac{\mu}{\triangle V}B_2^2\phi_\eta]_n-[\rho V\phi-\frac{\mu}{\triangle V}B_2^2\phi_\xi]_s \\ &=(S_\phi^C+\phi_p S_\phi^P)\triangle V+S_\phi^D \end{aligned} \tag{11}$$

where S_ϕ^D is the cross-derivative diffusion flux arising from the non-orthogonality of numerical grid and is treated explicitly as a source term to avoid the possibility of producing negative coeff-icients in an implicit treatment. It is defined as

$$S_\phi^D=\left(\frac{\mu}{\triangle V}B_2^1\phi_\eta\right)_e-\left(\frac{\mu}{\triangle V}B_2^1\phi_\eta\right)_w$$
$$+\left(\frac{\mu}{\triangle V}B_1^2\phi_\xi\right)_n-\left(\frac{\mu}{\triangle V}B_1^2\phi_\xi\right)_s \tag{12}$$

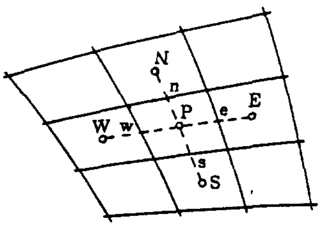

a) Physical plane

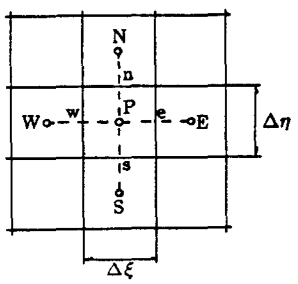

b) Transformed plane

Fig. 1 Finite difference grid representation in body-fitted coordinate system

The hybrid difference scheme is adopted, where the convective term is evaluated by first-order upwind differencing for $|P_e| > 2$ and by central differencing for $|P_e| \leq 2$. Central differencing is adopted for the diffusion terms. P_e denotes a Peclet number which is defined by $U\cdot J\cdot\delta\xi/(\mu\cdot B_1^1)$.

Finally, the discretized equation can be obtained as follows:

$$A_P\phi_P=A_E\phi_E+A_W\phi_W+A_N\phi_N+A_S\phi_S+b_\phi \tag{13}$$

where

$$A_P=A_E+A_W+A_N+A_S-S_\phi^P\triangle V$$
$$b_\phi=S_\phi^C+S_\phi^D.$$

A's are coefficients describing the influence of the neighbouring nodes surrounding the central node P, and contain contributions from the conv-ection and normal diffusion. Eq.(13) should be under-relaxed implicitly in order to achieve num-erical stability.

Momentum Interpolation Method

Calculation of velocities on the face of control volume is very important when the Navier-Stokes equations are solved in a general coordinate system. After some manipulation of the discretized Navi-er-Stokes equations of Eqs.(12) and (13), face velocities are calculated by

$$u_w^n=f_w^-[u_{i-1,j}^n+\alpha_u(D_1^u)_{i-1,j}(P_e-P_w)_{i-1,j}]$$
$$+f_w^+[u_{i,j}^n+\alpha_u\cdot(D_1^u)_{i,j}\cdot(P_e-P_w)_{i,j}]$$
$$-\alpha_u\cdot(\overline{D}_1^u)_w\cdot(P_P-P_W)$$
$$+(1-\alpha_u)\cdot[u_w^{n-1}-f_w^-\cdot u_{i-1,j}^{n-1}-f_w^+\cdot u_{i,j}^{n-1}] \tag{14}$$

where

α ; under-relaxation factor

$(D_1^u)_{i,j}=(y_\eta/A_p^u)_{i,j}$

$(\overline{D}_1^u)_w=(y_\eta)_w\cdot[f_w^+/(A_p^u)_{i,j}+f_w^-/(A_p^u)_{i-1,j}]$

f_w^+, f_w^- ; parameters of linear interpolation

The superscripts n, u denote n-th iteration and u-momentum equation, respectively, and the sub-scripts i, j denote index number of nodal points. And the overbar denotes the results obtained from linear interpoloation between the grid nodes, v_w^n, u_s^n and v_s^n can be calculated in the same way.

Pressure correction equation

There is no governing equation to obtain the pressure field directly. So the equation for pressure can be obtained by combining the solution of the continuity equation and momentum equations. SIMPLE Algorithm[12], [13] is used to solve the pressure field. The guessed pressure p^* should be improved in order that the resulting starred velocity field may progressively get closer to satisfy the continuity equation. The corrected pressur p is obtained from

$$p=p^*+p' \tag{15}$$

where p' is pressure correction. The corresponding velocity correction u', v' can be written in the same manner.

$$u=u^*+u' \tag{16}$$

$$v=v^*+v' \tag{17}$$

Substituting the Eqs.(15), (16) and (17) into the discretized momentum equations, Eq.(13), the velocity correction is obtained as:

$$u'_w=-\alpha_u \cdot (\overline{D}_1^u)_w \cdot (P'_p-P'_w) \tag{18}$$

$$u'_s=-\alpha_u \cdot (\overline{D}_2^u)_s \cdot (P'_p-P'_s) \tag{19}$$

In order to obtain the pressure correction equation, Eqs.(16), (17), (18) and (19) are substituted into the discretized continuity equation,

$$A_P \cdot P'_P=A_E \cdot P'_E+A_W \cdot P'_W+ A_N \cdot P'_N+A_S \cdot P'_S+F^* \tag{20}$$

where,

$A_E : \alpha_u \cdot (y_\eta)_e \cdot (\overline{D}_1^u)_e-\alpha_v \cdot (x_\eta)_e \cdot (\overline{D}_1^v)_e$

$A_W : \alpha_u \cdot (y_\eta)_w \cdot (\overline{D}_1^u)_w- \alpha_v \cdot (x_\eta)_w \cdot (\overline{D}_1^v)_w$

$A_N : \alpha_v \cdot (x_\xi)_n \cdot (\overline{D}_2^v)_n-\alpha_u \cdot (y_\xi)_n \cdot (\overline{D}_2^u)_n$

$A_S : \alpha_v \cdot (x_\xi)_s \cdot (\overline{D}_2^v)_s- \alpha_u \cdot (y_\xi)_s \cdot (\overline{D}_2^u)_s$

$A_P :\ A_E+A_W+A_N+A_S$

F^* : Net efflux over the control volume

After the pressure correction equation (20) is solved iteratively, the cell velocities are corrected by Eqs.(16) through (19) and the pressure is updated by Eq.(15).

Boundary Conditions

In order for a given problem to be well posed, boundary conditions for the solution domain are required, so that the resultant solution will be unique. The boundary conditions required for this problem are; Up-stream, Down-stream, Surface of the hydrofoil, External lateral and periodic boundary conditions. The physical domain, Fig. 2-(a), for a hydrofoil, is transformed to the computational domain, Fig. 2-(b). Details of the boundary conditions are as follows

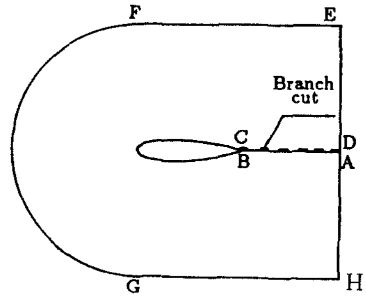

a) Physical domain.

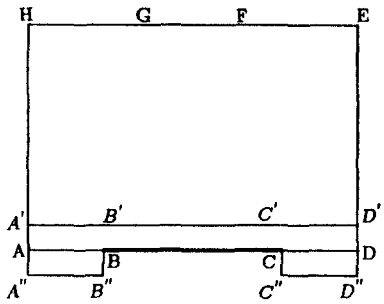

b) Transformed domain

Fig. 2 Solution domain for a hydrofoil

a) Up-stream(FG in Fig. 2)

$u=U_0 \cdot cos\alpha$

$v=U_0 \cdot sin\alpha$

where U_o is the oncoming total velocity and α is the angle of attack of the freestream.

b) Down-stream(AH, DE in Fig. 2)

$u_x = v_x = p_x = 0$

where the subscript denotes differentiation. The downstream boundaries are placed far enough from the hydrofoil such that the local flow of this down-stream has parabolic characteristics.

c) Surface of the hydrofoil(BC in Fig. 2)
Non-slip and impermeable conditions are imposed on the surface.

d) External lateral(EF, GH in Fig. 2)

$u = U_0 \cdot cos\alpha$

$p = 0$

The v-velocity component in this boundary is obtained from the law of mass conservation within the computational control volume during the solution procedure.

e) Periodic boundary(AB, CD in Fig. 2)

ϕ on the line A′B′ $= \phi$ on the line D′ C′
ϕ on the line C′D′ $= \phi$ on the line B′ A′

where ϕ is the dependent variable($=u$, v, p). This boundary condition should be well adapted to satisfy the conservation rule for all physical quantities because this boundary is a kind of branch cut. C-type grid needs this boundary condition.

Solution Procedure

The discretized differential equations with the above mentioned boundary conditions are solved iteratively. The solution algorithm is summarized briefly as follows:

i) Intermediate velocity components are obtained by solving the momentum Eq.(13), using the pressure field calculated at previous iteration.
ii) The cell-velocities are calculated using Eq. (14).
iii) The pressure correction equation is solved using Eq.(20).
iv) Intermediate face-velocities and centered velocities are updated using Eqs.(16) through (19). Also, intermediate pressure field is updated using the pressure correction Eq. (15).
v) Using these updated velocities and pressure, the whole procedure is repeated until a converged solation is obtained.

Each discretized governing equation is solved using a tridiagonal-matrix algorithm iteratively. Convergence is considered to be complete if the residual of the governing equations throughout the computation domain decreases to an infinitesimal value.

Numerical Grid

The advantages of curvilinear coordinates generated from the elliptic partial differential equations are the inherent smoothness that prevails in the solution of the elliptic systems, and the fact that some elliptic partial differential equations guarantee a one-to-one mapping between the physical and transformed domains. In the present study, the transformed poisson equations, initially proposed by Thompson et al.[14], [15], [16], are used,

$$\alpha \cdot x_{\xi\xi} - 2\beta \cdot x_{\xi\eta} + \gamma \cdot x_{\eta\eta} = -J^2(P \cdot x_\xi + Q \cdot x_\eta) \quad (21)$$

$$\alpha \cdot y_{\xi\xi} - 2\beta \cdot y_{\xi\eta} + \gamma \cdot y_{\eta\eta} = -J^2(P \cdot y_\xi + Q \cdot y_\eta) \quad (22)$$

where

$$x = x(\xi, \eta)$$
$$y = y(\xi, \eta)$$
$$\alpha = x_\eta^2 + y_\eta^2$$
$$\beta = x_\xi \cdot x_\eta + y_\xi \cdot y_\eta$$
$$\gamma = x_\xi^2 + y_\xi^2$$
$$J = x_\xi \cdot y_\eta - x_\eta \cdot y_\xi$$

The forcing functions P and Q are used as the controlling functions for contracting grids about a particular grid line [16]. The transformed Eqs.

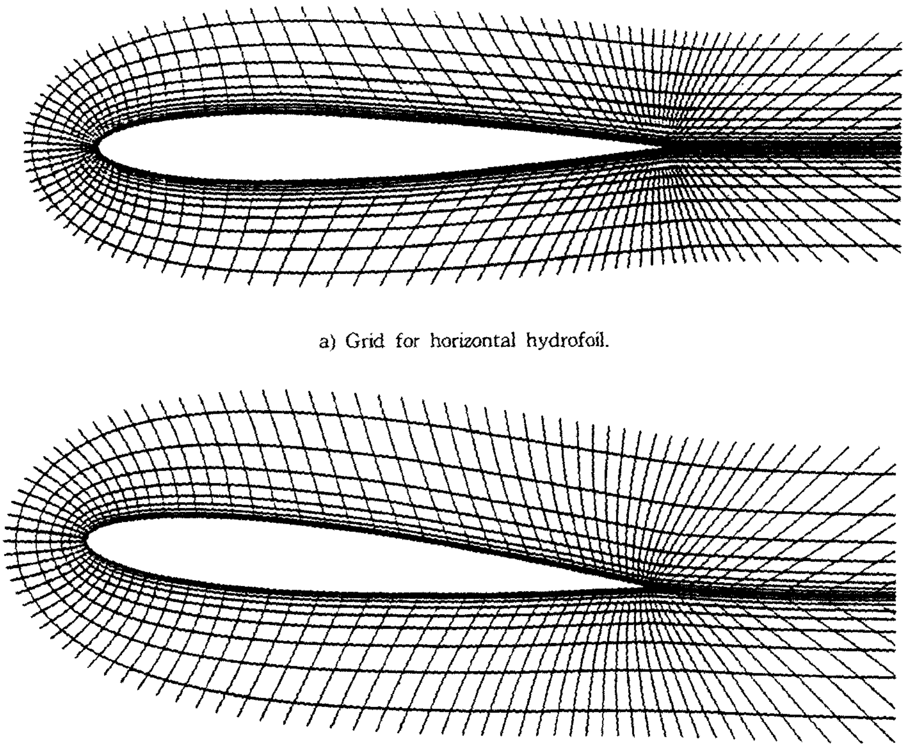

a) Grid for horizontal hydrofoil.

b) Grid for rotated hydrofoil by 5°

Fig. 3 Details of generated grid near body after reconstruction

(21) and (22), are easy to specify the boundary conditions for the contours. The generated grids is highly skewed in the wake region and have discontinuity in slope along the branch cut. In order to improve the quality of the generated grids, grid lines along the branch cut are recontracted using a cubic spline interpolation. The resulting grid are shown in Fig. 3.

4. Numerical Computations

A numerical code has been constructed and verified for the following computations.

Laminar flow results

The flow over a hydrofoil(NACA 0012) at zero incedence is computed when R_n=10,000. A total number of 154×70 grid points is used for the grid generation when 89 grid points were distributed on the hydrofoil surface. The upstream boundary is placed at a distance of 8.5 times the chord length from the leading edge. The boundaries at the downstream and external laterals are located at a distance of 10 times the chord length. The minimum grid spacing in the η-direction was 0.000798 times the chord length. Fig.3-(a) shows the grid system used.

The pressure distibution on the hydrofoil surface is plotted in Fig. 5. Comparisons of the present results with other results show good agreement even after the separation point. The results confirm that the present numerical scheme has sufficient accuracy to carry out other complex flow compu-

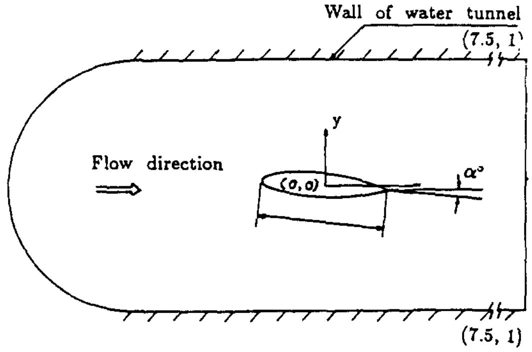

Fig. 4 Boundaries of the water tunnel used in numerical computation

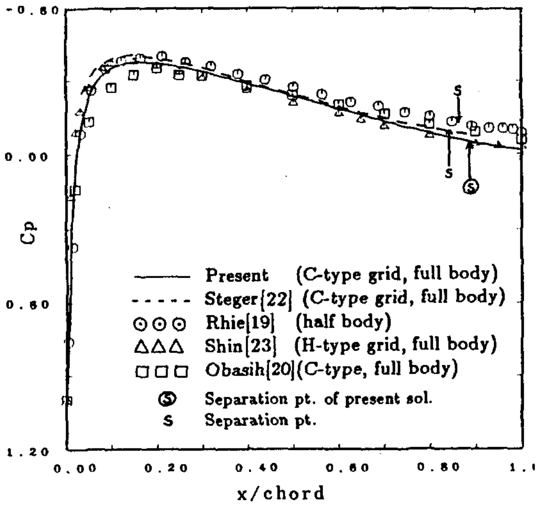

Fig. 5 Comparision of surface pressure coefficient distribution for NACA 0012 Foil, $R_N=10^4$ and $\alpha=0°$

tations. Fig. 6-(a), (b), (c) show the iso-pressure contours, streamlines and velocity vector, respectively. These results show good pressure-velocity coupling even though the C-type grid system has been used. Fig. 7 shows convergence history of the solution. Number of iterations to obtain the converged solution is dependent on the under-relaxation factor. About 300 iterations are required for convergence, which takes about 150 minutes in a personal computer(PC 386 with Weitek, 25MHz). Figs. 8 and 9 show the results for they hydrofoil with 5 degree angle of attack. The grid

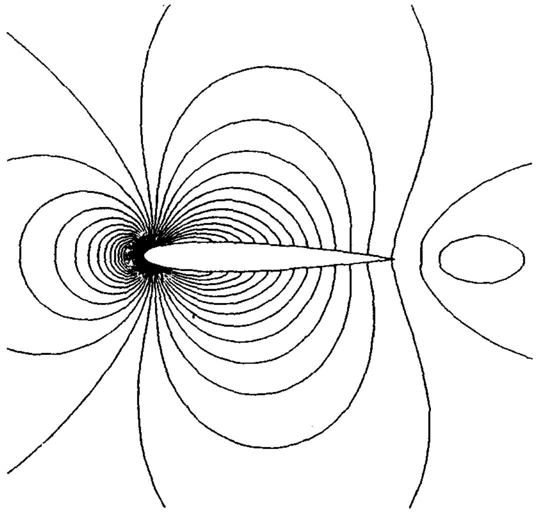

(a) Iso-pressure contour

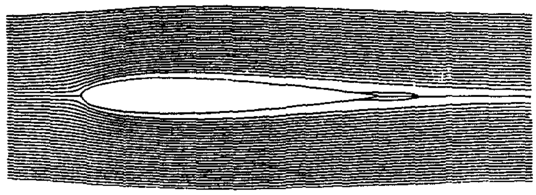

(b) Stream lines

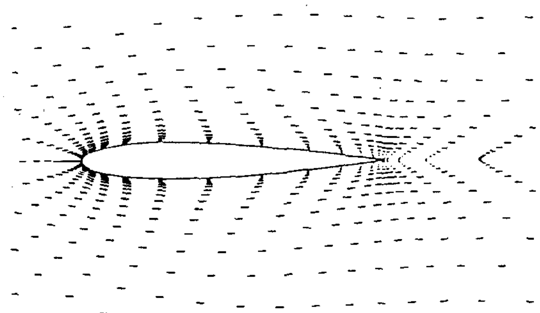

(c) Velocity vectors

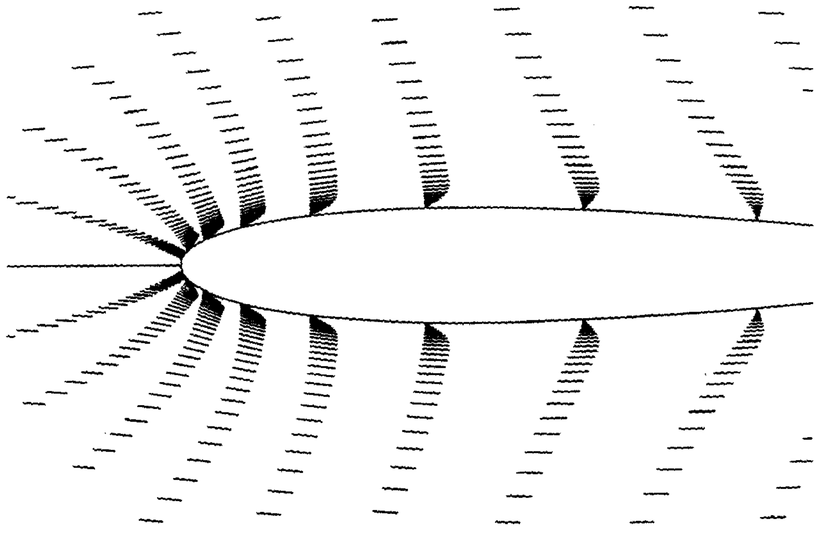

(d) Close-up of vel. vector around leading edge

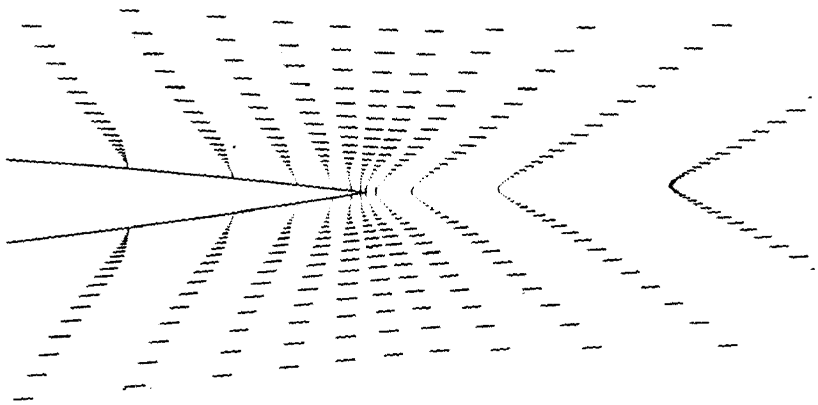

(e) Close-up of vel. vector around trailing edge

Fig. 6 Laminar flow for $R_N=10^4$ and $\alpha=0°$

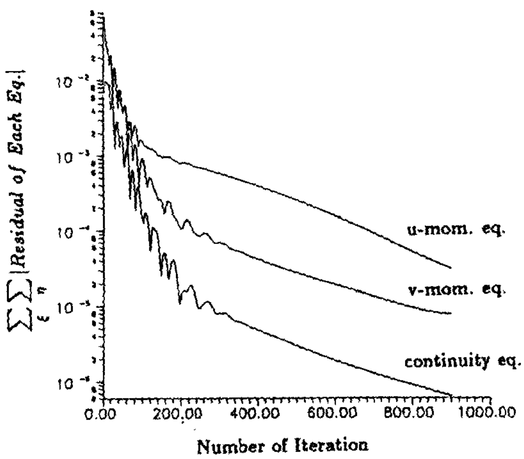

Fig. 7 Convergence history of governing equations ($R_N=10^4$, 0 incidence)

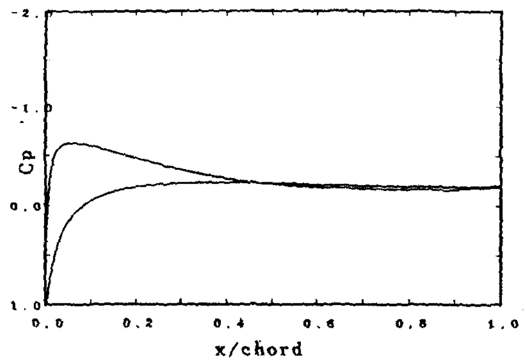

Fig. 8 Pressure coefficient distribution, $R_N=10^4$ and $\alpha=5°$

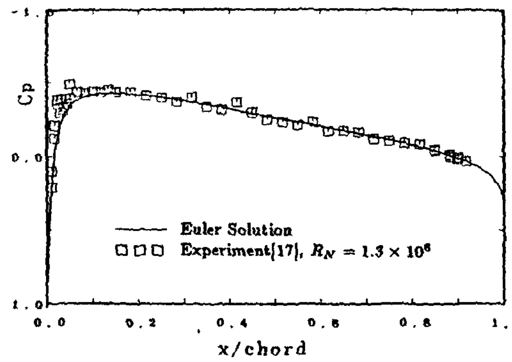

Fig. 10 Comparision of pressure coefficient distribution, $\alpha=0°$

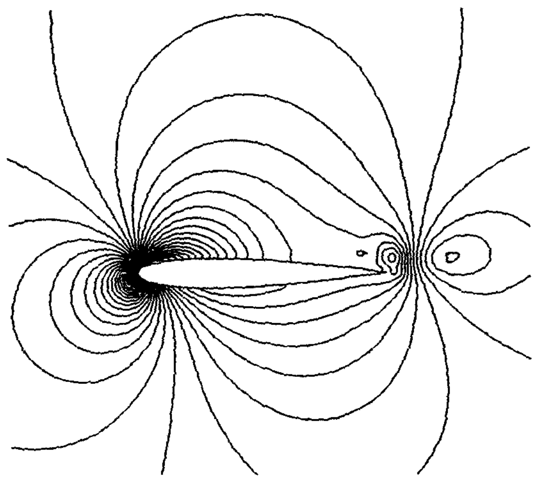

(a) Iso-pressure contrours

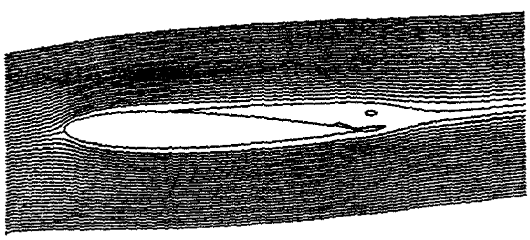

(b) Stream lines

Fig. 9 Laminar flow for $R_N=10^4$ and $\alpha=5°$

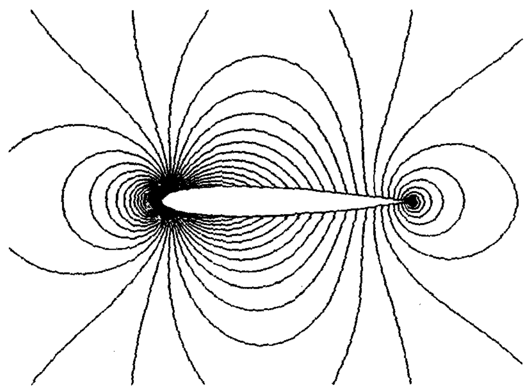

(a) Iso-pressure contrours

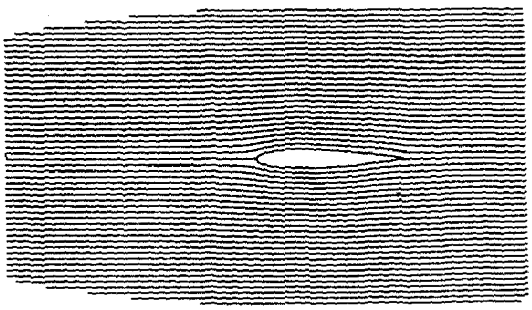

(b) Stream lines

Fig. 11 Euler solution considering the blockage effect of tunnel wall, $\alpha=0°$

system and all boundary conditions are the same as before. Laminar separation is found at a distance of 35% chord-fraction from the leading edge.

Euler solution results

The effects of viscosity on the surface pressure field is small if Reynolds number is high and the hydrofoil is operating at zero angle of attack. In order to validate the code, solution to the Euler equation, absent of the viscous terms in Eq.(2), is compared with the experimental data[17] at high Reynolds number.

In order to simulate the experimental conditions, the grid considering the wall of the water tunnel was generated. The boundaries of the physical domain are depicted in Fig. 4. Boundary layer development on the tunnel wall was neglected and slip boundary condition was applied on the wall surface. Fig. 10 shows the pressure distribution on the surface of the hydrofoil when angle of attack is 0 degree. Where qualitatively good agreements with the experimental data is found. Fig. 11(a), (b) shows the iso-pressure contours and streamlines, respectively.

5. Conclusions

Computational method for the calculation of the recirculating laminar flow in general body-fitted coordinate system was developed. The checkerboard instability, usually encountered when the non-staggered grid system is used, is removed by applying the momentum interpolation method. The computer program developed in the present study is useful for solving the engineering problems involving complex geometries, such as hydrofoils.

6. Acknowledgment

The work described in this paper was carried out under the sponsorship of the Ministry of Science and Technology, KOREA.

References

[1] Hirt, C.W., Amsden, A.A., and Cook, J.L., "An Arbitrary Lagrangian-Eulerian Computing Method for All Flow Speeds", *J. Comput. Phys.*, 17, 1974.

[2] Maliska C.R., and Raithby G.D., "A Method for Computing Three Dimensional Flows Using Non-Orthogonal Boundary-Fitted Coordinates", *International J. for Numerical Methods in Fluids*, Vol.4, 1984.

[3] Gosman A.D., and Ideriah F.J.K., "TEACH-2E : A General Computer Program for Two-Dimensional, Turbulent, Recirculating Flows", June, 1976.

[4] Shy Y.W., Tong S.S. and Correa S.M., "Numerical Recirculating Flow Calculation Using a Body-Fitted Coordinate System", *Numerical Heat Transfer*, Vol.8, 1985.

[5] Karaki K.C. and Patankar S.V., "Calculation Procedure for Viscous Incompressible Flows in Complex Geometries", *Numerical Heat Transfer*, Vol.14, 1988.

[6] Demirdzic I. A., "A Finite Volume Method for Computation of Fluid in Complex Geometries", *Ph.D. Thesis, University of London*, Oct. 1982.

[7] Rhie C.M. and Chow W.L., "Numerical Study of the Turbulent Flow Past and Airfoil with Trailing Edge Separation", *AIAA*, Vol.21, No. 21, Nov.1983.

[8] Majunder S., "Role of Under-relaxation in Momentum Interpolation for Calculation of Flow with Nonstaggered Grids", *Numerical Heat Transfer*, Vol.13, 1988.

[9] Miller T.F. and Schmidt F.W., "Use of a Pressure-Weighted Interpolation Method for the Solution of the Incompressible Navier-Stokes Equations on a Nonstaggered Grid System", *Numerical Heat Transfer*, Vol.14, 1988.

[10] Milovan Peric, "A Finite Volume Method for the Prediction of Three-Dimentional Fluid Flow in Complex Ducts", *Ph.D Thesis, University of*

London, August 1985.

[11] Hsu C.F., "A Curvilinear Coordinate Method for Momentum, Heat and Mass Transfer in Domains of Irregular Geometry", *Ph.D Thesis, University of Minesota*, 1981.

[12] Patankar Suhas V., "Numerical Heat Transfer and Fluid Flow", McGraw-Hill, New York, 1980.

[13] Patankar S.V. and Spalding D.B., "A Calculation Procedure for Heat, Mass and Momentum Transfer in Three-dimensional Parabolic Flows", *Int. J. Heat Transfer*, Vol.15, 1972.

[14] Thompson Joe F. Wars Z.U.A. and Mastin C. Wayne., "Numerical Grid Generation Foundation and Applications", 1985.

[15] Thompson, J.S. Thames F.C. and Mastin C.W., "Automatic Numerical Generation of Body-fitted Curvilinear Coordinate System For a Field Containing Any Number of Arbitrary Two-Dimensional Bodies", *J. Comp. Physics*, Vol.15, 1974.

[16] Steger, J.L. and Sorenson, R.L., "Automatic Mesh-Point Clustering Near a Boundary in Grid Generation with Elliptic Parial Differential Equations", *J. Computational Physics*, Vol.33, Dec. 1979.

[17] Ahn Jong-Woo and Kim Ki-Sup, Lee Jin-Tae., "Measurement of the Velocity, Pressure, Force and Moment about the NACA 0012 Hydrofoil", *Journal of Ship & Ocean Engineering Research*, Korea Research Institute of Ships & Ocean Engineering, Vol.2, Dec. 1989.

[18] Chen C.J. and Choi S.K., "The Finite Analytic Method and It's Applications : Laminar and Turbulent Flows Past Two Dimensional and Axisymmetric Bodies", *IIHR Report* No.334-I. The University of Iowa, March 1990.

[19] Rhie C.M., "A Numerical Study of the Flow Past and Isolated Airfoil with Separation", *Ph.D Thesis, University of Illinois*, 1981.

[20] Obasih K.M. and Chen C.J., "Prediction of Laminar and Turbulent Flows Past Single and Twin Hydrofoils", *IIHR Report No.317, The University of Iowa, Dec.* 1987.

[21] Acharya S. and Moukalled, F.H., "Improvement of Incompressible Flow Calculation on a Nonstaggered Curvilinear Grid", *Numerical Heat Transfer, Part B*, Vol.15, 1989.

[22] Steger, J.L., "Implicit Finite Difference Simulation of Numerical Recirculating Flow about Arbitrary Two-Dimensional Geometries", *AIAA J.* Vol.16, 1978.

[23] Shin, Myung-Soo., "Numerical Simulation of 2-Dimensional Sub-Breaking Waves by Finite Difference Method", *Ph.D Thisis, Hiroshima University*, 1989.